TITLE: Neurons Responsive to Global Visual Motion Have Unique Tuning Properties in Hummingbirds

AUTHORS: Andrea H. Gaede, Benjamin Goller, Jessica P.M. Lam, Douglas R. Wylie, Douglas L. Altshuler

JOURNAL: Current Biology

PUBLISHER: Elsevier

PUBLICATION DATE: 5 January 2017

DOI: 10.1016/j.cub.2016.11.041

Current Biology

Neurons responsive to global visual motion have unique tuning properties in hummingbirds

--Manuscript Draft--

Manuscript Number:	CURRENT-BIOLOGY-D-16-01093R2
Full Title:	Neurons responsive to global visual motion have unique tuning properties in hummingbirds
Article Type:	Report
Corresponding Author:	Douglas Altshuler University of British Columbia Vancouver, CANADA
First Author:	Andrea Holden Gaede
Order of Authors:	Andrea Holden Gaede
	Benjamin Goller
	Jessica Lam
	Douglas R Wylie
	Douglas Altshuler
Abstract:	Neurons in animal visual systems that respond to global optic flow exhibit selectivity for motion direction and/or velocity. The avian lentiformis mesencephali (LM), known in mammals as the nucleus of the optic tract (NOT), is a key nucleus for global motion processing [1-4]. In all animals tested, it has been found that the majority of LM and NOT neurons are tuned to temporo-nasal (back-to-front) motion [4-11]. Moreover, the monocular gain of the optokinetic response is higher in this direction, compared to naso-temporal (front-to-back) motion [12,13]. Hummingbirds are sensitive to small visual perturbations while hovering, and drift to compensate for optic flow in all directions [14]. Interestingly, the LM, but not other visual nuclei, is hypertrophied in hummingbirds relative to other birds [15], which suggests enhanced perception of global visual motion. Using extracellular recording techniques, we found that there is a uniform distribution of preferred directions in the LM in Anna's hummingbirds, whereas zebra finch and pigeon LM populations, as in other tetrapods, show a strong bias toward temporo-nasal motion. Furthermore, LM and NOT neurons are generally classified as tuned to "fast" or "slow" motion [10,16,17], and we predicted most neurons would be tuned to slow visual motion as an adaptation for slow hovering. However, we found the opposite result: most hummingbird LM neurons are tuned to fast pattern velocities, compared to zebra finches and pigeons. Collectively, these results suggest a role in rapid responses during hovering, and in velocity control and collision avoidance during forward flight of hummingbirds.

Neurons responsive to global visual motion have unique tuning properties in hummingbirds

Andrea H. Gaede,[1] Benjamin Goller,[1] Jessica P.M. Lam,[1] Douglas R. Wylie,[2] and Douglas L. Altshuler[1]*

1. Department of Zoology, University of British Columbia, Vancouver, BC, Canada, V6T 1Z4
2. Centre for Neuroscience and Department of Psychology, University of Alberta, Edmonton, AB, Canada, T6G 2E9

* To whom correspondence should be addressed. Email: doug@zoology.ubc.ca

Summary:

Neurons in animal visual systems that respond to global optic flow exhibit selectivity for motion direction and/or velocity. The avian lentiformis mesencephali (LM), known in mammals as the nucleus of the optic tract (NOT), is a key nucleus for global motion processing [1–4]. In all animals tested, it has been found that the majority of LM and NOT neurons are tuned to temporo-nasal (back-to-front) motion [4–11]. Moreover, the monocular gain of the optokinetic response is higher in this direction, compared to naso-temporal (front-to-back) motion [12,13]. Hummingbirds are sensitive to small visual perturbations while hovering, and drift to compensate for optic flow in all directions [14]. Interestingly, the LM, but not other visual nuclei, is hypertrophied in hummingbirds relative to other birds [15], which suggests enhanced perception of global visual motion. Using extracellular recording techniques, we found that there is a uniform distribution of preferred directions in the LM in Anna's hummingbirds, whereas zebra finch and pigeon LM populations, as in other tetrapods, show a strong bias toward temporo-nasal motion. Furthermore, LM and NOT neurons are generally classified as tuned to "fast" or "slow" motion [10,16,17], and we predicted most neurons would be tuned to slow visual motion as an adaptation for slow hovering. However, we found the opposite result: most hummingbird LM neurons are tuned to fast pattern velocities, compared to zebra finches and pigeons. Collectively, these results suggest a role in rapid responses during hovering, and in velocity control and collision avoidance during forward flight of hummingbirds.

Results:

We made extracellular recordings from the LM of hummingbirds and zebra finches while presenting large-field random dot patterns in the contralateral visual field (Figure 1A). LM neurons receive direct retinal input, and show simple direction selectivity across large, but restricted, receptive fields. We used a random dot-field, rather than a more complex stimulus, because more complicated patterns of optic flow are processed downstream [18,19]. LM neurons were spontaneously active and exhibited motion opponency, defined as increased firing in response to large-field stimulus motion in a “preferred” direction, and decreased firing in the opposite, “anti-preferred,” direction [4,16,17,20].

We first identified the preferred direction of LM neurons by presenting visual motion in each of eight directions, 45° apart. Each motion stimulus lasted 5 s, and was bounded by 5 s pauses. Raw extracellular recordings are shown for one hummingbird cell during a full trial (Figure 1A), and two zebra finch cells during a portion of a trial, with higher temporal resolution (Figure 1D). Single units were isolated offline using amplitude or template spike sorting (Figures 1E,F; S1B; supplementary methods).

Individual neurons were defined as directionally tuned if the response to direction was significantly non-uniform (Rayleigh test). The total sample size of directionally tuned neurons was 152 units from ten zebra finches, and 88 units from six hummingbirds. Thirteen out of 165 (7.8%) zebra finch cells, and eight out of 96 (8.3%) hummingbird cells, were not direction-modulated, which is similar to the percentage of non-directional cells previously reported in pigeons [4,21,22]. For comparison, we also

analyzed data from 100 LM units in 38 pigeons, from previous studies in which moving large-field sine wave gratings were used as visual stimuli [1,4,23–25]. Because speed tuning width is maintained for some but not all visual motion neurons when comparing responses to sine wave gratings and random dot fields [26], we limited our comparison with pigeon data to just preferred direction and preferred speed.

Directional tuning curves are shown for one hummingbird cell (Figure 1B) and two zebra finch cells (Figure 1F). Mean firing rate is plotted as a function of the direction of motion in polar coordinates (forward = 0°, down = -90°, up = 90°, backward = ±180°; Figure S1A; supplementary methods). An analysis of the direction tuning width is also included in the supplementary materials (Figure S2).

Most zebra finch LM cells prefer temporo-nasal motion (0° in our coordinate system) as is the case for pigeons (Figure 2). A Rayleigh test confirmed that these two distributions were non-uniform (both $P < 0.0001$). In contrast, most hummingbird neurons are tuned to other directions such that at the population level, the distribution of preferred directions is uniform (Rayleigh test $P = 0.379$). We determined confidence intervals for the population direction preference by bootstrapping the data within each species (Figure 2D-F). This analysis confirms overall direction preferences of LM populations for zebra finches and pigeons, but not for hummingbirds. Thus, the uniform distribution observed in hummingbird LM neurons is unique relative to zebra finches, pigeons and indeed all other tetrapods studied to date.

We next examined LM activity in response to visual motion speed (Figure 3). Cellular responses were measured in both preferred and anti-preferred directions over a

range of speeds (0.24, 0.5, 1, 2, 4, 8, 16, 24, 32, 48, 64, 80°/s; presented in random order) similar to other experiments with birds (LM) and mammals (NOT) [4,6,10,16,17,20,27,28]. Each motion sweep lasted 5 s, and was bounded by 5 s pauses. Because recording sites were tested at a single pair of directions, but some measured multiple neurons with different preferred directions, we had to remove cells from further analysis. Only LM cells measured in their preferred direction ±45° were included in the speed analysis, leading to sample sizes of 56 and 107 units in hummingbirds and zebra finches, respectively. Speed tuning curves were calculated as the mean of five trials.

The responses of neurons to visual motion speed can, in principle, be categorized by both tuning width and speed preference. We estimated the width of tuning curves for each cell by summing the number of velocity values that elicited a firing rate above a given percentage of the maximum firing rate (e.g., # bins above 50% of max rate) versus that threshold (e.g., 50%) (Figure 3D). Differences between hummingbird and zebra finch cells were first tested using a linear mixed effects model, but because we found a significant interaction between threshold and species ($F_{1,1465}$=107.207, P < 0.0001), we next fit a linear model to each species separately. The slope of the relationship between the numbers of speed bins above threshold and the threshold is more negative in zebra finches (-9.92; y-intercept = 11.45) than in hummingbirds (-6.66; y-intercept = 7.59), and the lines do not converge over the meaningful range (thresholds up to 100% of maximum firing). Thus, within the range of velocities tested, hummingbird LM cells exhibit high relative levels of response for fewer speed bins than zebra finch neurons. The distributions of the number of speed bins

above 70, 80, and 90 percent thresholds, as well as bootstrapped data for the speed tuning width (number of consecutive speed bins) at 80 percent of maximum firing rate are presented in Figure S3 A-D.

From the tuning curves we also calculated the speed preference of each neuron. We first described the speed preference as a single value – the speed at which maximum firing was achieved (Figure 3E). The hummingbird and zebra finch data are plotted along with similar data from pigeons. It is important to reiterate that the data from our study are derived from experiments using moving dot-fields, whereas the pigeons were tested with sinusoidal gratings. In addition, the speed test values do not overlap completely. The average value for the pattern speed with the highest firing rate across the three cell populations increased from pigeons to zebra finches to hummingbirds. Despite an average preference for higher stimulus velocities, hummingbirds had a larger proportion of the relatively low number of slow cells recorded. In hummingbirds, 20% of the LM population (11 cells) prefers speeds < 6°/s, but the majority, 80% of the population (45 cells), prefer speeds > 6°/s. Conversely, in zebra finches, only 4% of the population (4 cells) prefers speeds < 6°/s, and 96% (103 cells) prefers speeds > 6°/s. However, we did not observe strong evidence for distinct populations of “fast” and “slow” LM neurons.

We next considered the overall response of the LM neuron population to increasing motion speeds. When accounting for neurons responding at near maximal levels for multiple motion speeds, the LM responses of both hummingbirds and zebra finches appear to saturate over the range of speeds tested and we did not measure a subsequent decline. The saturating response is illustrated in figure 3F, which depicts

the data for neurons responding with at least 80% of their maximum firing rate. Figure S3 (E-F) provides the data for 70% and 90% of maximum firing. We fit sigmoidal curves to the hummingbird and zebra finch LM population responses to increasing speeds, allowing slope or inflection point parameters to vary by cell. Comparisons of the fitted parameters for the two species indicate that hummingbird LM cells show a strong preference for high-velocity visual motion. Responses of zebra finch LM cells to increasing speed saturate more quickly (higher slope, $F_{1,14} = 26.78$; $P < 0.0001$) and at lower stimulus velocities (inflection point at lower speed, $F_{1,14} = 25.86$; $P < 0.001$). Because we did not test higher speeds, we cannot exclude the possibility that hummingbird LM neurons are high pass rather than band pass filters. Regardless, the hummingbird LM response is significantly shifted toward higher motion speeds.

A notable feature of the speed tuning curves was a difference in the extent of overall excitation and suppression between zebra finch and hummingbird LM neurons (examples in Figure S4). To determine if this difference was significant, we quantified the level of excitation and suppression as the area under each of the two speed tuning curves (one for each direction) for each unit. Plotting the area under the anti-preferred direction tuning curve versus the area of the preferred direction curve leads to three plausible options for how relative firing rate of a neuron can encode visual motion preference. Values greater than zero indicate overall excitation, whereas negative values indicate overall suppression. Thus, the lower right quadrant of Figure 4A includes LM cells that were excited in the preferred direction and suppressed in the anti-preferred direction relative to the spontaneous firing rate. An example of a zebra finch neuron with these firing characteristics is provided in Figure 4C. The upper right

quadrant contains cells that were excited in both directions, and an example cell from a zebra finch is depicted in Figure 4B. The lower left quadrant contains cells that were suppressed in both directions, and an example cell from a hummingbird is provided in Figure 4D. The upper left quadrant contains no cells by definition because the preferred direction is defined by higher relative firing.

At the population level, while still overlapping, hummingbird and zebra finch LM neurons are shifted apart along the suppression-excitation axes (Figure 4A). Hummingbird LM neurons have significantly lower excitation (smaller area under the curve) in the preferred direction ($F_{1,14} = 35.91$; $P < 0.0001$), and significantly greater suppression in the anti-preferred direction ($F_{1,14} = 8.09$; $P = 0.013$) compared to zebra finch LM neurons.

Discussion:

Hovering hummingbirds are highly sensitive to coherent background motion in all directions in their visual field, and adjust their three-dimensional position to compensate for this motion [14]. This strong response to global motion direction was not matched with a tuned response to changes in stimulus pattern speed, though only a few pattern speeds were tested [14]. Heightened sensitivity, during hovering flight, to direction rather than velocity suggests that hummingbirds have neural specializations to detect global motion direction stimuli.

The LM is a pretectal nucleus and one of two midbrain nuclei associated with the accessory optic system (AOS) that process global motion direction and velocity. The LM is hypertrophied in hummingbirds and enlarged, but to a lesser extent, in transiently

hovering species [15]. This enlargement may represent a neural specialization related to hovering flight. Iwaniuk and Wylie (2007) proposed that a greater relative number of LM neurons preferring slow speeds could aid stabilization during hovering [15]. The goals of the present study were to test this hypothesis and also determine whether the direction preferences of the hummingbird LM conform to the tetrapod pattern.

Previous studies with tetrapods have demonstrated that the direction preferences of LM neurons, or neurons in the homologous NOT, are biased towards temporo-nasal motion. For example, a [^{14}C]2-deoxyglucose study in chicks has shown increased glucose uptake in LM cells during motion in the temporo-nasal direction [3]. Furthermore, in pigeons, 53% of recorded LM cells preferred forward (temporo-nasal) motion, whereas the remaining cell preferences were distributed amongst backward, downward, and upward motion [4]. This bias is consistent with other pigeon LM data [10,20,29], and across other tetrapod species, including chicks [3], turtles [30], frogs [31,32], salamanders [33], wallabies [7], rabbits [34], and cats [6]. It is less clear whether this holds for optic-flow-sensitive neurons in the pretectum of fish, which do not show the same bias for temporo-nasal motion observed in the tetrapod LM or NOT [35–38]. The current study demonstrates that hummingbird LM neurons deviate strongly from the tetrapod pattern by having no directional bias at the population level (Figure 2).

LM neurons are further characterized as being selective for velocity, with a preference for either “slow” or “fast” speeds [10], and exhibiting a correlation between temporo-nasal direction preference and slow speed preference [4,17]. Using large-field grating patterns in pigeons, fast cells prefer low spatial frequencies (SF) and high temporal frequencies (TF), whereas slow cells prefer high SF and low TF [1,4,16]. Other

previous studies, which used random dot-fields in pigeons, classified 82% of measured LM cells as “fast” (>6°/s), and 18% as “slow” (<6°/s) [17]. If we apply this threshold (6°/s), we find that 20% of hummingbird LM neurons are “slow” cells, while only 4% of zebra finch LM neurons had maximal firing at a slow velocity. Compared to zebra finches, we found that hummingbird LM neurons are more selective for a preferred speed over the range of velocities we tested, and prefer faster visual motion (Figure 3). Although the percentage of “slow” cells based on a 6°/s threshold is similar in hummingbirds and pigeons, we did not observe a clear distinction between fast and slow LM neuron populations in either zebra finches or hummingbirds. Moreover, when previously published pigeon data are presented in the same manner (Figure 3E), there is no obvious bimodal distribution for this species either. This is likely due to spatio-temporal, rather than velocity, tuning [4].

The LM has a reciprocal relationship with the nucleus of the basal optic root (nBOR) of the AOS; both are retinal-recipient midbrain nuclei and project to each other. Unlike the population-level preference for temporo-nasal motion observed in the pigeon and zebra finch LM (Figure 2), studies in pigeons show that nBOR neurons prefer upward, downward, and naso-temporal motion, with very few cells (~5-10%) preferring temporo-nasal motion [1,39]. Similar direction preference distributions have been shown in the nBOR of turtles [40] and chickens [41]. Furthermore, the nBOR is homologous to the mammalian medial and lateral terminal nuclei of the AOS [5,8,42], which contain direction-sensitive neurons that respond best to vertical motion [43–45]. In mammals, the AOS also contains the dorsal terminal nuclei, which have cells that respond preferentially to horizontal motion [45,46]. The complementary LM-nBOR relationship is

further demonstrated by their responses to global motion direction; the LM receives inhibitory inputs from slow nBOR cells that prefer motion of the opposite direction.

Compared to zebra finches, hummingbird LM neurons are more suppressed by motion in the anti-preferred direction and less excited by motion in the preferred direction (Figure 4). The strong inhibition of hummingbird LM neurons by motion in the anti-preferred direction (Figure 4A) could be attributed to an nBOR-mediated mechanism that drives speed tuning (i.e., disinhibition of nBOR). The expansion of the direction preference distribution that we found in the hummingbird LM suggests that the complementary relationship observed in pigeons between the LM and nBOR is not apparent, or may not function in the same way, in hummingbirds.

The ability to sustain hovering flight in hummingbirds is unique among vertebrates. The motion preferences and firing properties of LM neurons are also distinct from all other tetrapods in several respects, which supports the hypothesis that hummingbirds have neural specializations for flight mode [15]. The uniform distribution of direction preferences in the hummingbird LM is unique among all tetrapods studied to date, and in combination with their preference for faster speeds, suggests heightened sensitivity to global motion at high speeds. Such sensitivity could be beneficial during hovering when birds are close to visual features that will produce high global motion velocity in response to even small changes in position. This specialization may also play a role in more dynamic behaviors such as competitive interactions, high-speed courtship displays and insect foraging [47–49]. Testing this hypothesis will require moving to visual stimuli relevant to more complex flight modes [50] and in higher order brain centers [11,51].

Experimental Procedures:

We used standard extracellular recording techniques to study the LM of anesthetized birds while presenting a computer-generated moving dot-field to the contralateral eye (Figure 1A,C; Figure 3A). Details of the surgical and recording procedures, visual stimulus, and statistical approaches are provided in the Supplemental Information. All spike-sorted data and analysis scripts are available via figshare (URL will be available after acceptance).

Experimental subjects included ten adult male zebra finches (*Taeniopygia guttata*; Eastern Bird Supplies, Quebec, Canada), six adult male Anna's hummingbirds (*Calypte anna*; caught on the University of British Columbia campus, October 2014 – April 2015). All experimental procedures were approved by the Animal Care Committee of the University of British Columbia.

Supplemental Information

Figure S1; Figure S2; Figure S3; Figure S4

Supplemental Experimental Procedures

For data and analysis, see the statistical supplement available here: (Link will be added upon final acceptance).

Author Contributions

A.H.G. and D.L.A. conceived and designed the experiment. A.H.G. and J.P.M.L. collected the data. A.H.G., B.G., and D.R.W. analyzed the data. A.H.G. and D.L.A. wrote the manuscript. All authors edited the manuscript.

Acknowledgements

We are grateful to four anonymous reviewers for constructive feedback on the manuscript. This study was supported by grants from the Natural Sciences and Engineering Research Council of Canada (402667) and the Human Frontier Science Foundation (RGP0003/2013).

References:

1. Crowder, N.A., Dawson, M.R.W., and Wylie, D.R.W. (2003). Temporal frequency and velocity-like tuning in the pigeon accessory optic system. J. Neurophysiol. *90*, 1829–1841.

2. Kuhlenbeck, H., and Miller, R.N. (1942). The pretectal region of the rabbit's brain. J. Comp. Neurol. *76*, 323–365.

3. Mckenna, O.C., and Wallman, J. (1981). Identification of avian brain regions responsive to retinal slip using 2-deoxyglucose. Brain Res. *210*, 455–460.

4. Wylie, D.R., and Crowder, N.A. (2000). Spatiotemporal properties of fast and slow neurons in the pretectal nucleus lentiformis mesencephali in pigeons. J. Neurophysiol. *84*, 2529–2540.

5. Fite, K.V. (1985). Pretectal and accessory optic visual nuclei of fish, amphibia and reptiles - theme and variations. Brain. Behav. Evol. *26*, 71–90.

6. Hoffmann, K., and Schoppmann, A. (1981). A quantitative analysis of the direction-specific response of neurons in the cat's nucleus of the optic tract. Exp. Brain Res. *42*, 146–157.

7. Ibbotson, M.R., Mark, R.F., and Maddess, T.L. (1994). Spatiotemporal response properties of direction-selective neurons in the nucleus of the optic tract and dorsal terminal nucleus of the wallaby, *Macropus eugenii*. J. Neurophysiol. *72*, 2927–2943.

8. Mckenna, O.C., and Wallman, J. (1985). Accessory optic system and pretectum of birds: Comparisons with those of other vertebrates. Brain. Behav. Evol. *26*, 91–116.

9. Mustari, M.J., and Fuchs, A.F. (1990). Discharge patterns of neurons in the pretectal nucleus of the optic tract (NOT) in the behaving primate. J. Neurophysiol. *64*, 77–90.

10. Winterson, B.J., and Brauth, S.E. (1985). Direction-selective single units in the nucleus lentiformis mesencephali. Exp. Brain Res. *60*, 215–226.

11. Wylie, D.R. (2013). Processing of visual signals related to self-motion in the cerebellum of pigeons. Front. Behav. Neurosci. *7*.

12. Gioanni, H. (1988). Stabilizing gaze reflexes in the pigeon (*Columba livia*) .1. Horizontal and vertical optokinetic eye (OKN) and head (OCR) reflexes. Exp. Brain Res. *69*, 567–582.

13. Eckmeier, D., and Bischof, H.-J. (2008). The optokinetic response in wild type and white zebra finches. J. Comp. Physiol. A *194*, 871–878.

14. Goller, B., and Altshuler, D.L. (2014). Hummingbirds control hovering flight by stabilizing visual motion. Proc. Natl. Acad. Sci. U. S. A. *111*, 18375–18380.

15. Iwaniuk, A.N., and Wylie, D.R.W. (2007). Neural specialization for hovering in hummingbirds: Hypertrophy of the pretectal nucleus lentiformis mesencephali. J. Comp. Neurol. *500*, 211–221.

16. Ibbotson, M.R., and Price, N.S.C. (2001). Spatiotemporal tuning of directional neurons in mammalian and avian pretectum: A comparison of physiological properties. J. Neurophysiol. *86*, 2621–2624.

17. Xiao, Q., and Frost, B.J. (2013). Motion parallax processing in pigeon (*Columba livia*) pretectal neurons. Eur. J. Neurosci. *37*, 1103–1111.

18. Graham, D.J., and Wylie, D.R. (2012). Zebrin-immunopositive and-immunonegative stripe pairs represent functional units in the pigeon vestibulocerebellum. J. Neurosci. *32*, 12769–12779.

19. Crowder, N.A., Winship, I.R., and Wylie, D.R. (2000). Topographic organization of inferior olive cells projecting to translational zones in the vestibulocerebellum of pigeons. J. Comp. Neurol. *419*, 87–95.

20. Fu, Y.X., Gao, H.F., Guo, M.W., and Wang, S.R. (1998). Receptive field properties of visual neurons in the avian nucleus lentiformis mesencephali. Exp. Brain Res. *118*, 279–285.

21. Wylie, D.R.W. (2000). Binocular neurons in the nucleus lentiformis mesencephali in pigeons: responses to translational and rotational optic flowfields. Neurosci. Lett. *291*, 9–12.

22. Gu, Y., Wang, Y., and Wang, S.R. (2001). Directional modulation of visual responses of pretectal neurons by accessory optic neurons in pigeons. Neuroscience *104*, 153–159.

23. Crowder, N.A., and Wylie, D.R. (2002). Responses of optokinetic neurons in the pretectum and accessory optic system of the pigeon to large-field plaids. J. Comp. Physiol. A Neuroethol. Sens. Neural. Behav. Physiol. *188*, 109–119.

24. Crowder, N.A., Lehmann, H., Parent, M.B., and Wylie, D.R.W. (2003). The accessory optic system contributes to the spatio-temporal tuning of motion-sensitive pretectal neurons. J. Neurophysiol. *90*, 1140–1151.

25. Crowder, N.A., Dickson, C.T., and Wylie, D.R.W. (2004). Telencephalic input to the pretectum of pigeons: an electrophysiological and pharmacological inactivation study. J. Neurophysiol. *91*, 274–285.

26. Priebe, N.J., Lisberger, S.G., and Movshon, J.A. (2006). Tuning for spatiotemporal frequency and speed in directionally selective neurons of macaque striate cortex. J. Neurosci. *26*, 2941–2950.

27. Distler, C., and Hoffmann, K.-P. (2011). Visual pathway for the optokinetic reflex in infant macaque monkeys. J. Neurosci. *31*, 17659–17668.

28. Volchan, E., Rochamiranda, C.E., Picancodiniz, C.W., Zinsmeisser, B., Bernardes, R.F., and Franca, J.G. (1989). Visual response properties of pretectal units in the nucleus of the optic tract of the opossum. Exp. Brain Res. *78*, 380–386.

29. Wylie, D.R.W., and Frost, B.J. (1996). The pigeon optokinetic system: Visual input in extraocular muscle coordinates. Vis. Neurosci. *13*, 945–953.

30. Fan, T.X., Weber, A.E., Pickard, G.E., Faber, K.M., and Ariel, M. (1995). Visual responses and connectivity in the turtle pretectum. J. Neurophysiol. *73*, 2507–2521.

31. Fite, K.V., Kweilevy, C., and Bengston, L. (1989). Neurophysiological investigation of the pretectal nucleus lentiformis mesencephali in *Rana pipiens*. Brain. Behav. Evol. *34*, 164–170.

32. Li, Z., Fite, K.V., Montgomery, N.M., and Wang, S.R. (1996). Single-unit responses to whole-field visual stimulation in the pretectum of *Rana pipiens*. Neurosci. Lett. *218*, 193–197.

33. Manteuffel, G. (1984). Electrophysiology and anatomy of direction-specific pretectal units in *Salamandra salamandra*. Exp. Brain Res. *54*, 415–425.

34. Collewijn, H. (1975). Direction-selective units in the rabbit's nucleus of the optic tract. Brain Res. *100*, 489–508.

35. Kubo, F., Hablitzel, B., Dal Maschio, M., Driever, W., Baier, H., and Arrenberg, A.B. (2014). Functional architecture of an optic flow-responsive area that drives horizontal eye movements in zebrafish. Neuron *81*, 1344–1359.

36. Masseck, O.A., and Hoffmann, K.-P. (2009). Question of reference frames: Visual direction-selective neurons in the accessory optic system of goldfish. J. Neurophysiol. *102*, 2781–2789.

37. Masseck, O.A., and Hoffmann, K.-P. (2008). Responses to moving visual stimuli in pretectal neurons of the small-spotted dogfish (*Scyliorhinus canicula*). J. Neurophysiol. *99*, 200–207.

38. Klar, M., and Hoffmann, K.-P. (2002). Visual direction-selective neurons in the pretectum of the rainbow trout. Brain Res. Bull. *57*, 431–433.

39. Gioanni, H., Rey, J., Villalobos, J., and Dalbera, A. (1984). Single unit-activity in the nucleus of the basal optic root (nBOR) during optokinetic, vestibular and visuo-vestibular stimulations in the alert pigeon (*Columba livia*). Exp. Brain Res. *57*, 49–60.

40. Rosenberg, A.F., and Ariel, M. (1990). Visual-response properties of neurons in turtle basal optic nucleus in vitro. J. Neurophysiol. *63*, 1033–1045.

41. Burns, S., and Wallman, J. (1981). Relation of single unit properties to the oculomotor function of the nucleus of the basal optic root (accessory optic system) in chickens. Exp. Brain Res. *42*, 171–180.

42. Simpson, J.I. (1984). The accessory optic system. Annu. Rev. Neurosci. *7*, 13–41.

43. Soodak, R.E., and Simpson, J.I. (1988). The accessory optic system of rabbit. I. Basic visual response properties. J. Neurophysiol. *60*, 2037–2054.

44. Grasse, K.L., and Cynader, M.S. (1982). Electrophysiology of medial terminal nucleus of accessory optic system in the cat. J. Neurophysiol. *48*, 490–504.

45. Grasse, K.L., and Cynader, M.S. (1984). Electrophysiology of lateral and dorsal terminal nuclei of the cat accessory optic system. J. Neurophysiol. *51*, 276–293.

46. Mustari, M.J., and Fuchs, A.F. (1989). Response properties of single units in the lateral terminal nucleus of the accessory optic system in the behaving primate. J. Neurophysiol. *61*, 1207–1220.

47. Segre, P.S., Dakin, R., Zordan, V.B., Dickinson, M.H., Straw, A.D., and Altshuler, D.L. (2015). Burst muscle performance predicts the speed, acceleration, and turning performance of Anna's hummingbirds. eLife *4*, e11159.

48. Stiles, F.G. (1982). Aggressive and courtship displays of the male Anna's hummingbird. Condor *84*, 208–225.

49. Stiles, F.G. (1995). Behavioral, ecological and morphological correlates of foraging for arthropods by the hummingbirds of a tropical wet. Condor *97*, 853–878.

50. Dakin, R., Fellows, T.K., and Altshuler, D.L. (2016). Visual guidance of forward flight in hummingbirds reveals control based on image features instead of pattern velocity. Proc. Natl. Acad. Sci. *113*, 8849–8854.

51. Frost, B.J. (2010). A taxonomy of different forms of visual motion detection and their underlying neural mechanisms. Brain. Behav. Evol. *75*, 218–235.

Figure Legends:

Figure 1. Representative data depicting preferred direction analysis. A: A representative raw trace of an extracellular recording of a hummingbird LM neuron. Arrows indicate direction of dot-field motion, broken lines indicate paused stimulus. The hummingbird illustration shows the bird's head orientation during stimulus presentation. B: A polar plot of the mean firing rate (spikes/s) in response to motion in each direction (green circles) for the neuron in A with a B-spline fit to the mean firing rates ±SE (thick magenta ± thin). The gray line indicates spontaneous activity (spikes/s). F = forward motion (temporo-nasal), U = up, B = backward (naso-temporal), D = down. C: A portion of a raw extracellular recording of a zebra finch LM. D: A zoomed in portion of the trace in panel C with spikes from two different neurons (red, blue) sorted from the raw trace (black). E: An overlay of the average waveforms of 20 consecutive spikes (± SEM) for each of the two classes of spikes identified in D. PCA cluster analysis for these two cells is provided in figure S1B. F: Polar plots for the direction-modulated response for each cell in panel D. Red and blue lines are means ±SE, gray = spontaneous activity. Direction tuning width analysis is provided in figure S2.

Figure 2. Hummingbird LM cells have a uniform distribution of preferred directions, whereas zebra finches and pigeons prefer forward motion. A-C: Individual cell analysis. Rosette plots show the distribution of preferred directions within the recorded LM populations. Each colored circle represents the preferred direction of a single cell. The circular distributions of preferred directions are calculated as two von Mises parameters: μ the location of central tendency on the circle, and κ, a descriptor of the concentration at that location. For zebra finches, μ was 6.02° ± 5.761° (95% CI:

8.74° to 2.65°) and κ: was 1.24 ± 0.148. For pigeons, μ was -7.63° ± 11.57° (95% CI: -5.5° to -9.2°) and κ was 0.722 ± 0.155. The hummingbird LM population has a uniform distribution. D-F: Population analysis. We resampled with replacement the responses of individual neurons 1000 times each, to generate 1000 LM cell populations for each species. Each circle represents the preferred direction of an entire LM population that passed the Rayleigh test. In hummingbirds (D), 21/1000 populations had a preferred direction, always generally downward. In zebra finches (E),1000/1000 populations were non-uniform with population direction preference (μ) of 5.71° ± 0.061°, and concentration (κ) of 898.3. In pigeons (F),1000/1000 populations were non-uniform with population direction preference (μ) of -7.31° ± 0.041°, and concentration (κ) of 1998. Bird illustrations indicate the head orientation.

Figure 3. **Hummingbird LM neurons prefer higher visual motion speed than zebra finches LM neurons**. A representative raw trace shows an extracellular recording from the zebra finch LM during the velocity tuning experiment (A). Arrows indicate direction of dot-field motion; broken lines indicate paused stimulus. The zebra finch illustration shows orientation of the bird's head during stimulus presentation. Representative velocity tuning curves for a hummingbird (B) and a zebra finch (C) LM cell depict normalized firing rate (±SEM) plotted against the stimulus velocity (log scale) in the preferred (black squares) and anti-preferred directions (gray diamonds). The dashed gray line indicates a threshold of 80% of the maximum firing rate. Box plots of grouped data (D) depict the number of speed bins at successive thresholds (percentages) of the maximum firing rate for hummingbirds (magenta triangles) and zebra finches (orange circles). Magenta and orange diamonds indicate mean. Speed preferences of LM

neurons are plotted using two different criteria: (E) the proportion of the LM population for each species that reaches maximal firing at a given stimulus velocity (a single value for each cell); (F) the proportion of the LM cells that have a firing rate above 80% of their maximum firing rate at each stimulus velocity. Figure S3 provides supplemental visualizations of velocity tuning width analysis and speed preference plots showing the proportion of the LM population responding at additional percentages of the maximum firing rate.

Figure 4. **Hummingbird LM cells are less excited than zebra finch cells by motion in their preferred direction, and are more suppressed by motion in their anti-preferred direction.** The magnitude of excitation and suppression is calculated as the area under the velocity tuning curve (AUC) in response to motion in the preferred and anti-preferred directions, respectively. The two AUC values are plotted against each other with error bars (SD) calculated from AUCs for 1000 bootstrapped simulations of each cell's responses (A). Representative velocity tuning plots (B,C,D) demonstrate mean response (±SEM) to motion in the preferred (black squares) and anti-preferred (gray diamonds) directions of cells that fall into quadrants b, c, and d, respectively. In some cases, the error bars are occluded by the symbol at a given response value. Magenta triangles = hummingbird LM cells; orange circles = zebra finch LM cells. Further examples of speed tuning curves are provided in figure S4.

Figure 1

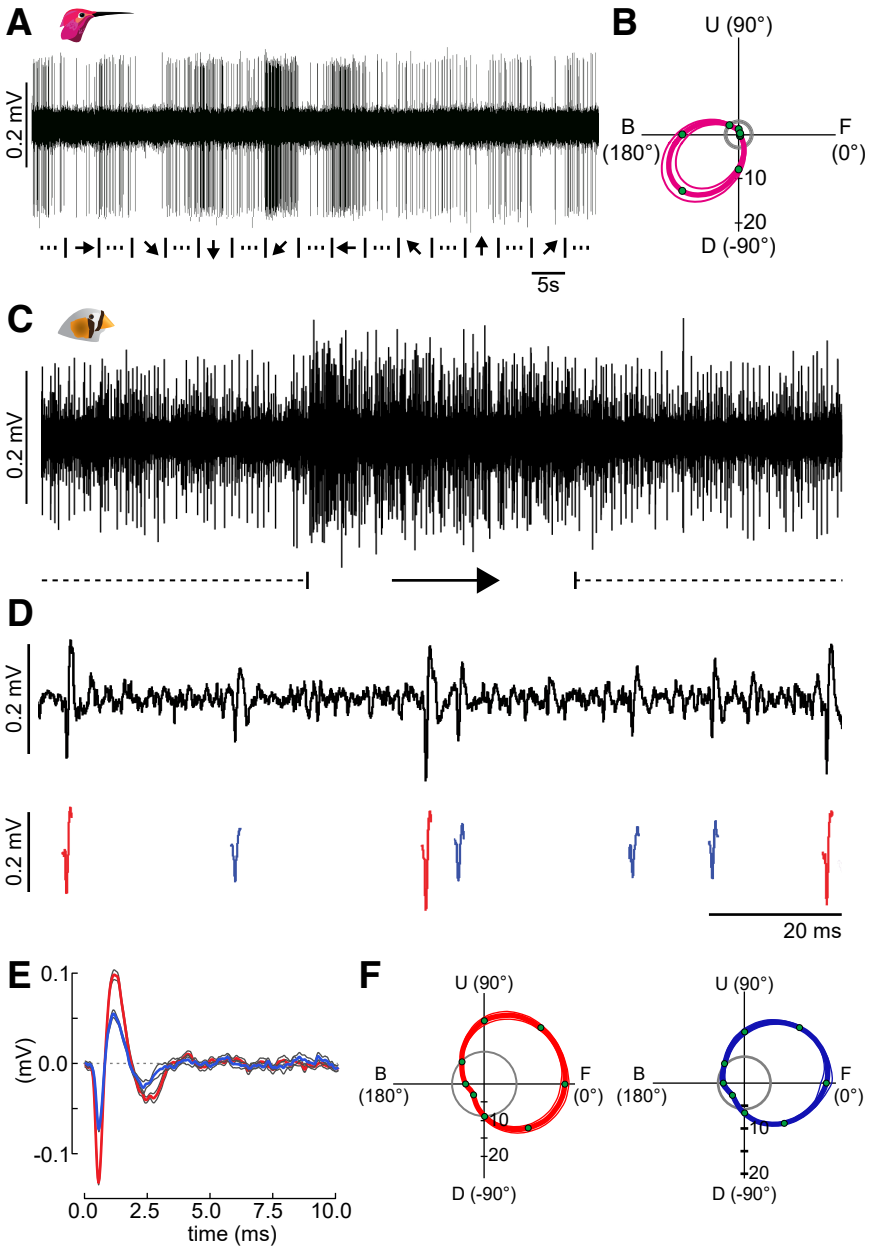
A
0.2 mV
5s
B
U (90°)
B (180°)
F (0°)
10
20
D (-90°)
C
0.2 mV
D
0.2 mV
0.2 mV
20 ms
E
0.1
(mV)
0.0
-0.1
0.0
2.5
5.0
7.5
10.0
time (ms)
F
U (90°)
B (180°)
F (0°)
10
20
D (-90°)
U (90°)
B (180°)
F (0°)
10
20
D (-90°)

Figure 2

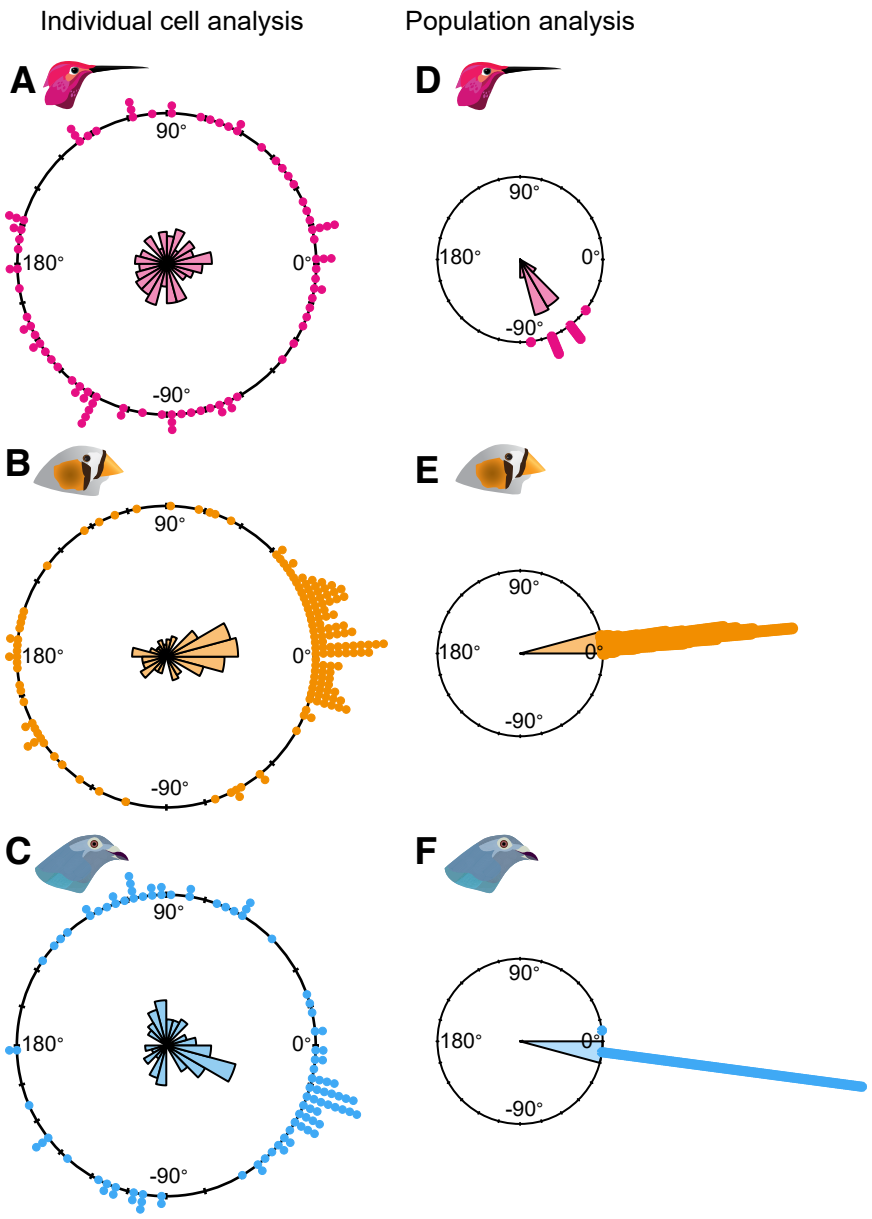
Individual cell analysis
Population analysis
A
B
C
D
E
F
90°
180°
0°
-90°

Figure 3

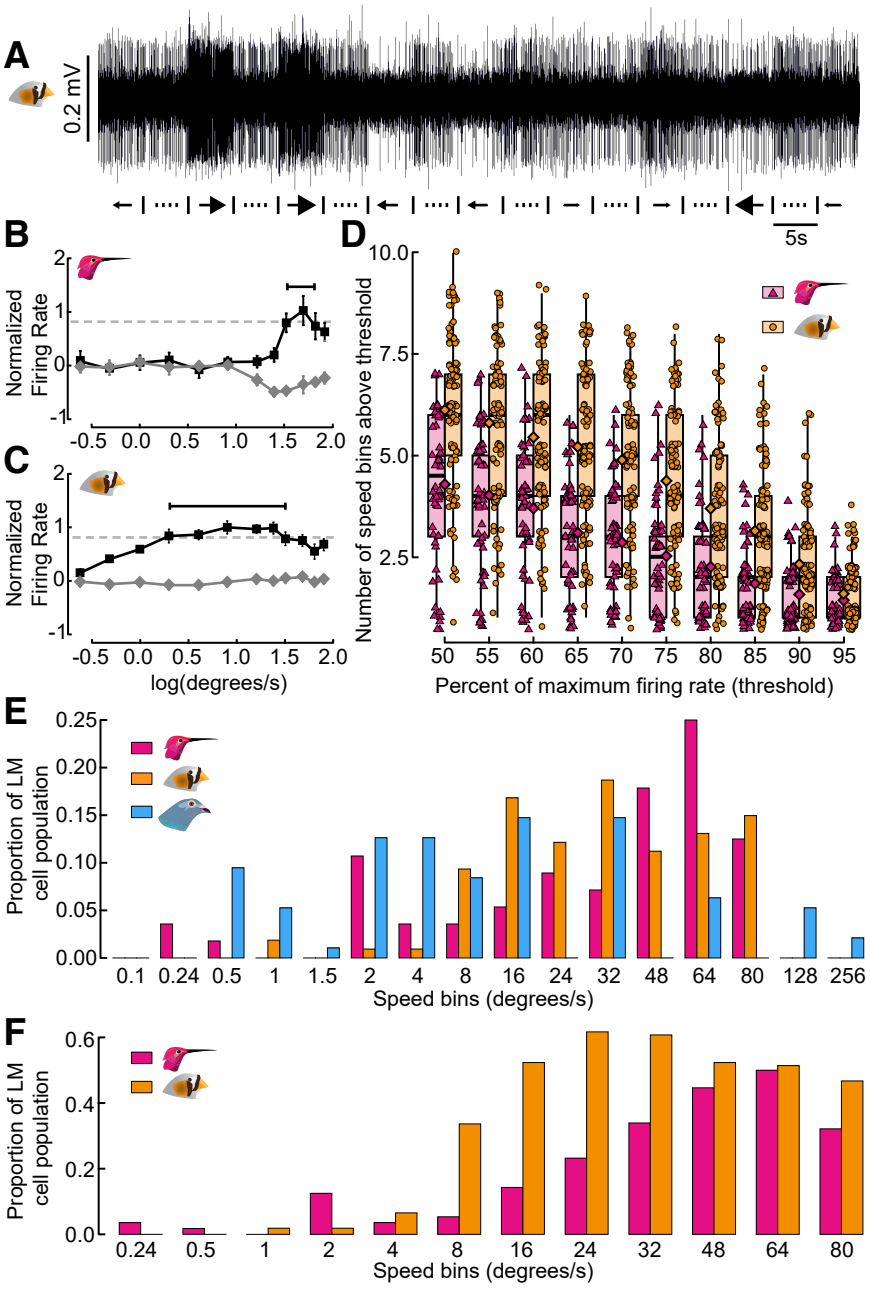
A
0.2 mV
5s
B
Normalized Firing Rate
C
Normalized Firing Rate
log(degrees/s)
D
Number of speed bins above threshold
Percent of maximum firing rate (threshold)
E
Proportion of LM cell population
Speed bins (degrees/s)
F
Proportion of LM cell population
Speed bins (degrees/s)

Figure 4

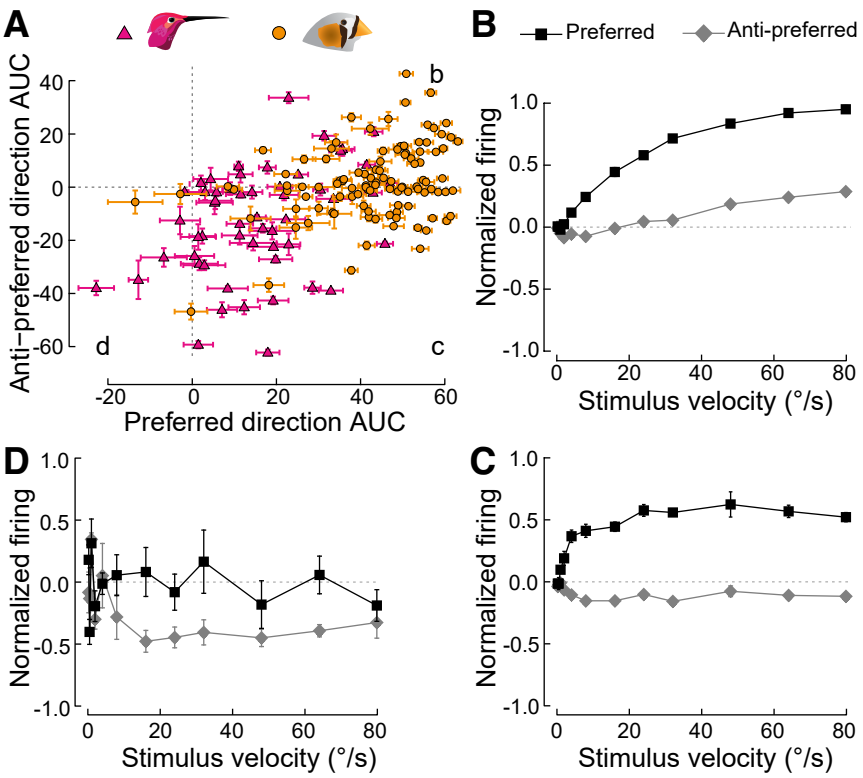
A
B
Preferred
Anti-preferred
b
d
c
Anti−preferred direction AUC
Preferred direction AUC
Normalized firing
Stimulus velocity (°/s)
D
C

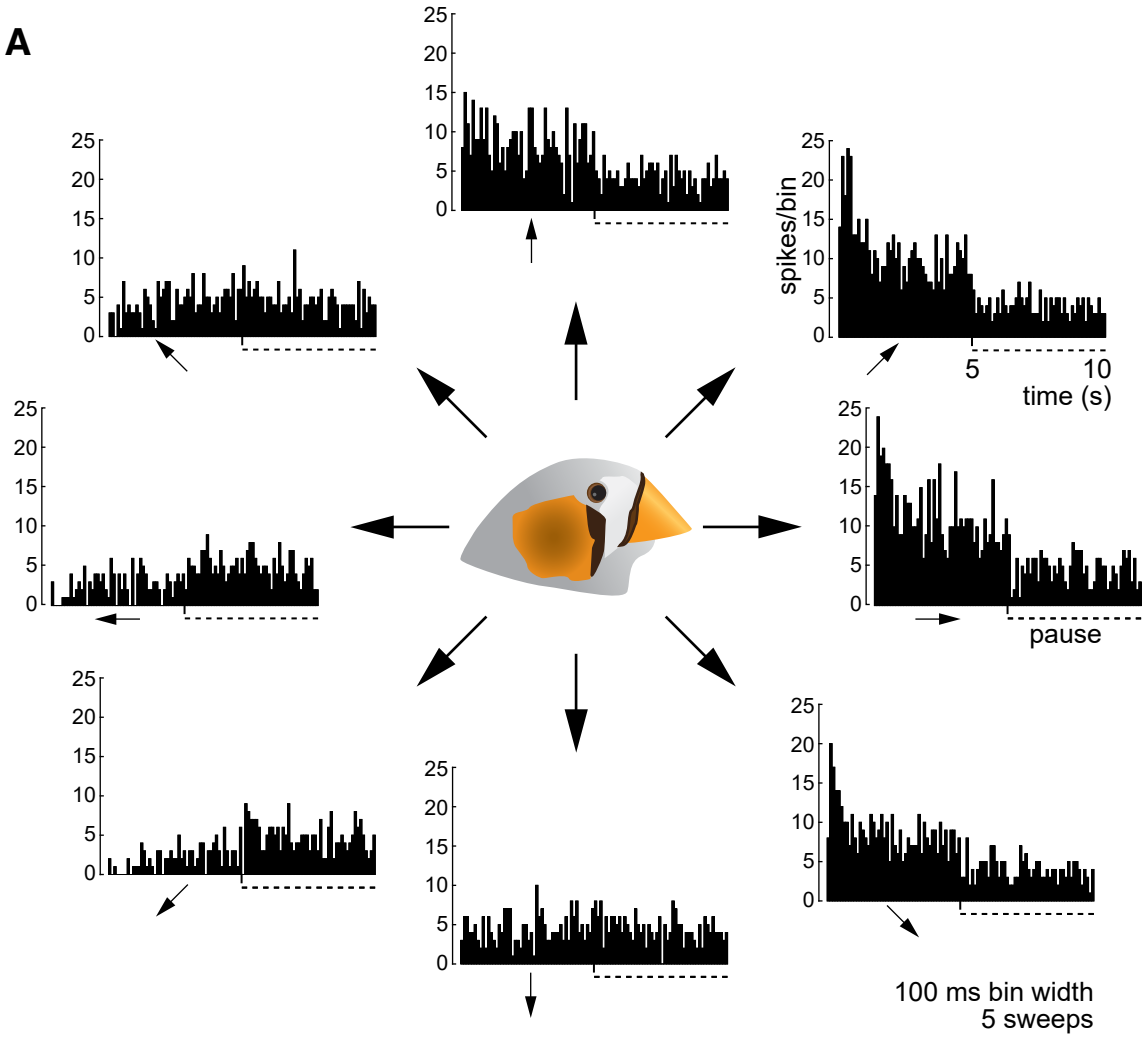
A
spikes/bin
time (s)
pause
100 ms bin width
5 sweeps

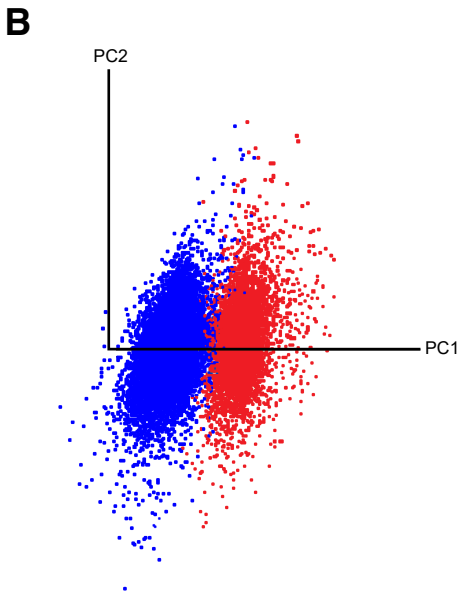
B
PC2
PC1

Figure S1. ***Related to figure 1*. Peristimulus time histograms depicting responses of a single zebra finch cell to motion in eight directions and subsequent pauses.** A: Peristimulus time histograms (PSTHs) in response to each direction of motion for a zebra finch LM neuron. Each PSTH is the sum of 5 sweeps (100 ms bin width). For each sweep, there was 5 s of motion in one direction (arrow), followed by a 5 s pause (dashed line). The zebra finch head illustration indicates the head orientation relative to the motion direction indicated by arrows in the PSTHs. B: PCA cluster analysis of the two cells shown in Figure 1D-E.

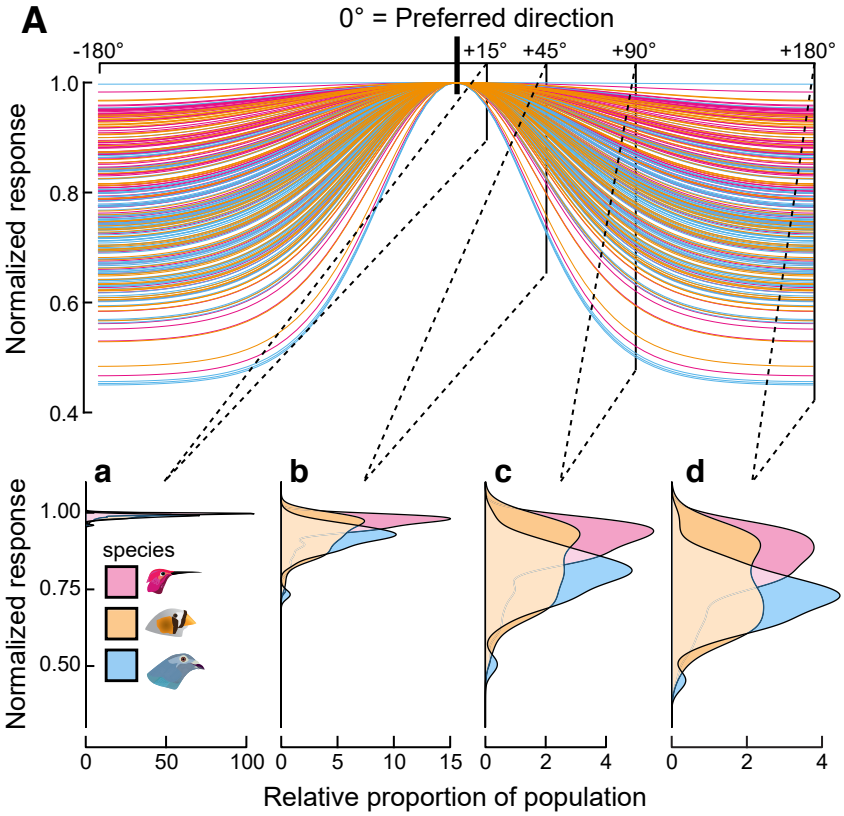
A
0° = Preferred direction
-180°
+15°
+45°
+90°
+180°
1.0
0.8
0.6
0.4
Normalized response
a
b
c
d
1.00
0.75
0.50
Normalized response
species
0
50
100
0
5
10
15
0
2
4
0
2
4
Relative proportion of population

Figure S2. ***Related to figure 1*. The direction tuning curves indicate that there is no difference in direction tuning width at angles less than ±45° from the preferred direction.** A: Differences in preferred direction tuning width between hummingbirds, zebra finches and pigeons is illustrated by plotting the von Mises distribution fit to each LM neuron, and aligning the preferred directions (center parameter μ) so that differences in relative shape can be observed. Hummingbird curves are magenta; zebra finch curves are orange; pigeon curves are blue. Subpanels a-d plot the normalized firing rate versus relative proportion of the LM population (for each species) at given angles from the preferred direction, which is normalized to 0°.

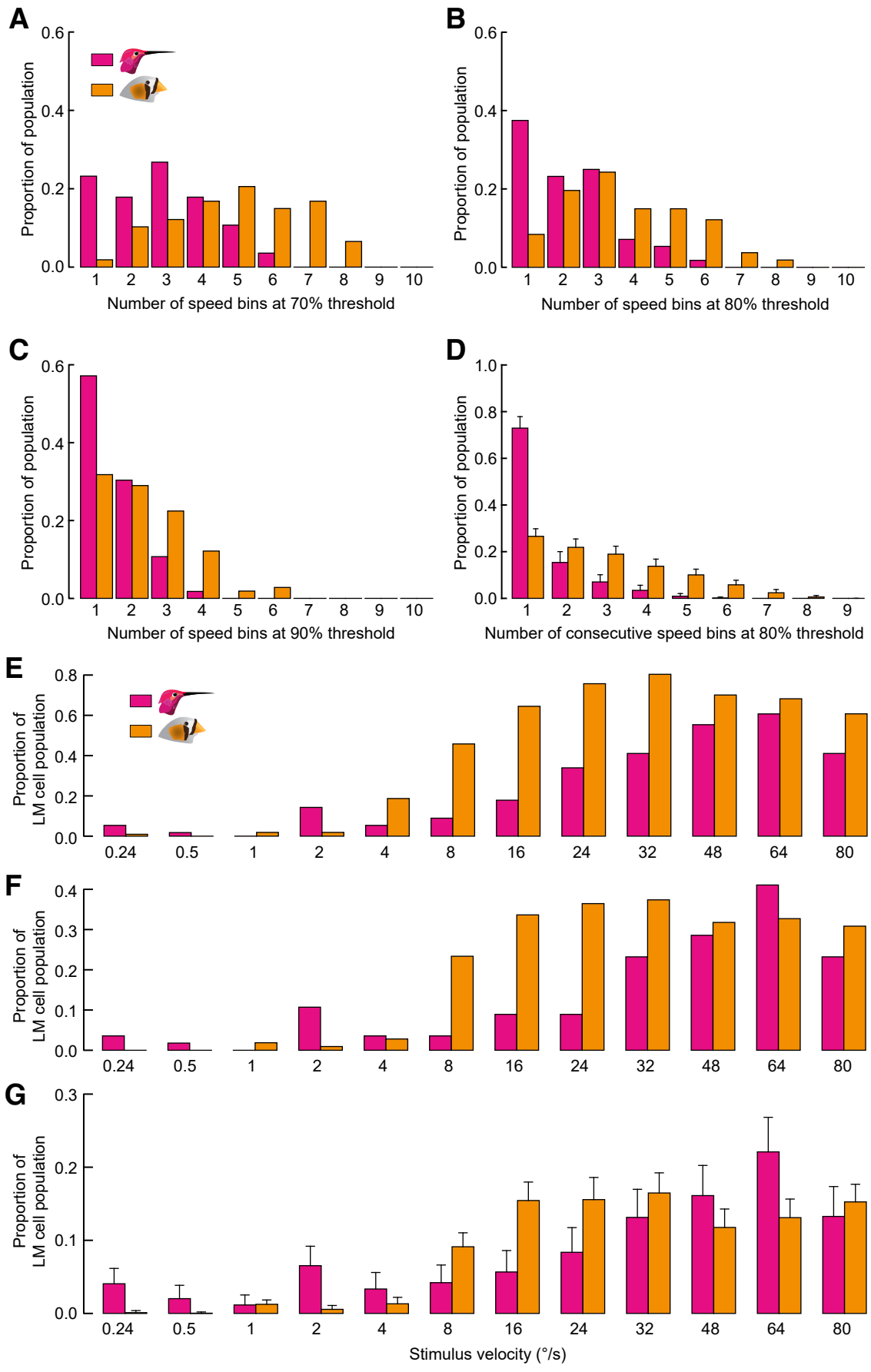
A
Proportion of population
0.0
0.2
0.4
0.6
1 2 3 4 5 6 7 8 9 10
Number of speed bins at 70% threshold
B
Proportion of population
0.0
0.2
0.4
0.6
1 2 3 4 5 6 7 8 9 10
Number of speed bins at 80% threshold
C
Proportion of population
0.0
0.2
0.4
0.6
1 2 3 4 5 6 7 8 9 10
Number of speed bins at 90% threshold
D
Proportion of population
0.0
0.2
0.4
0.6
0.8
1.0
1 2 3 4 5 6 7 8 9
Number of consecutive speed bins at 80% threshold
E
Proportion of LM cell population
0.0
0.2
0.4
0.6
0.8
0.24 0.5 1 2 4 8 16 24 32 48 64 80
F
Proportion of LM cell population
0.0
0.1
0.2
0.3
0.4
0.24 0.5 1 2 4 8 16 24 32 48 64 80
G
Proportion of LM cell population
0.0
0.1
0.2
0.3
0.24 0.5 1 2 4 8 16 24 32 48 64 80
Stimulus velocity (°/s)

Figure S3. ***Related to figure 3*. Supplement to velocity tuning width analysis and preferred speed data**. The proportion of the LM population at each ‘number of speed bins above threshold’, using a 70% (A), 80% (B), and 90% (C) of maximum firing rate threshold. Bootstrapping the velocity tuning width data (number of consecutive speed bins) at the 80% threshold gives confidence intervals (1000 populations). Means plus standard error are plotted (D). The preferred speed analysis is expanded by examining the proportion of the hummingbird (magenta) and zebra finch (orange) LM populations that fire at rates greater than 70% (E) and 90% (F) of maximum firing at each stimulus speed. Bootstrapping the preferred velocity data using the 80% of maximum firing threshold (1000 populations) provides confidence intervals for these data for both species (G).

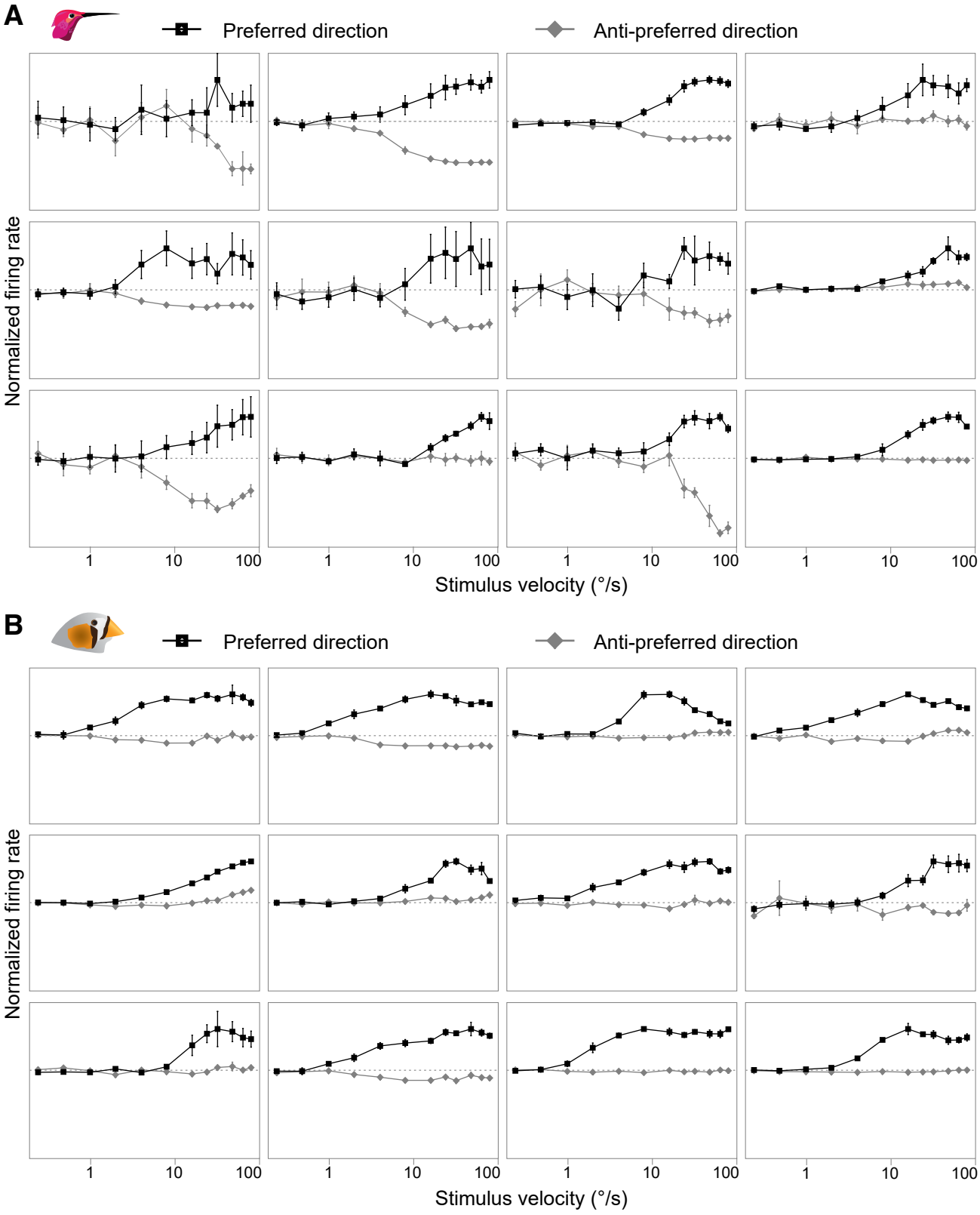
A
Preferred direction
Anti-preferred direction
Normalized firing rate
1
10
100
Stimulus velocity (°/s)
B
Preferred direction
Anti-preferred direction
Normalized firing rate
1
10
100
Stimulus velocity (°/s)

Figure S4. ***Related to figure 4*. A series of representative speed tuning curves for hummingbird (A) and zebra finch (B) LM cells.** Mean firing rate ±SEM (normalized to max excitation) is plotted against stimulus velocity. Black squares = response to motion in preferred direction; gray diamonds = response to motion in the anti-preferred direction.

Supplemental Experimental Procedures:

Animals.

All experimental procedures were approved by the University of British Columbia Animal Care Committee in accordance with the guidelines set out by the Canadian Council on Animal Care. Experimental subjects included ten adult male zebra finches (*Taeniopygia guttata*; Eastern Bird Supplies, Quebec, Canada), six adult male Anna's hummingbirds (*Calypte anna*; caught on the University of British Columbia campus, October 2014 – April 2015).

We focused on hummingbirds because this clade has hypertrophied LM nuclei, which is hypothesized to be neural specialization for their hovering flight. We selected *C. anna* because there is considerable information available about its retinal and brain anatomy [S1,S2], as well as its visually-guided flight behavior [S3–S5]. We compared *C. anna* with data we collected for *T. guttata* because zebra finches are small songbirds that also have high wingbeat frequency [S6]. The analysis also includes similar data from pigeons that were collected in a previous study [S7–S11], which we included because this species is the dominant model for visual neuroscience studies in birds.

Although these three species have different foraging behavior and some difference in flight modes, they have generally similar performance in at least some metrics. The maximum flight speeds obtained in wind tunnels are 12-14 m/s for different hummingbird species [S12–S14], 12-14 m/s for zebra finches [S15–S17], and up to 20 m/s for pigeons [S18]. The maximum flight speeds during courtship dives in

hummingbirds are 27 m/s [S19], but to our knowledge similar data for the presumed maximum speeds of zebra finches and pigeons are not currently available.

Anna's hummingbirds and zebra finches have similar eye sizes. The transverse diameter of *C. anna* eyes is 5.33 ± 0.49 mm [S20] and *T. guttata* eyes is 5.8 to 6.8 mm [S21]. Thus we do not expect major differences in velocity tuning due to eye size difference [S22].

Surgery and electrophysiological recording procedures.

Each bird was anesthetized by intramuscular injection in the pectoral muscles with a ketamine/xylazine mixture (zebra finch: 65 mg/kg ketamine / 8 mg/kg xylazine; hummingbird: 50 mg/kg ketamine / 8 mg/kg xylazine). Supplemental doses were administered as required. Subcutaneous injections 0.9% saline were given to maintain fluids. Once anesthetized, birds were placed in a custom-built stereotaxic frame (Herb Adams Engineering, Glendora, CA, USA) with ear bars and an adjustable beak bar suitable for both species. In hummingbirds, the ear bars were inserted into the external auditory meatus to firmly hold the skull so that the brain could be positioned in accordance with unpublished histological studies in the Anna's hummingbird. The LM coordinates were calculated using serial photomicrographs of fixed, Nissl stained brain sections. In zebra finches, the ear bars were pinned against the otic process of the quadrate bone, which lies in the anterior part of the opening to the external acoustic meatus. This allowed for positioning of the head in accordance with the stereotaxic atlas of the zebra finch brain (Konishi, unpublished). The head was angled downwards at an angle of 45° to the horizontal plane. Using these coordinates, sufficient bone and dura

mater overlying the right telencephalon were removed to expose the surface of the brain and allow access to the LM in the vertical axis.

Extracellular recordings were made using glass micropipettes filled with 2 M NaCl and having tip diameters of 8-10 µm (outer diameter). The signal was amplified (×10,000; A-M Systems, Inc., Model 3000 differential amplifier; Sequim, WA), band pass filtered (0.1 – 3 kHz), sampled at 30 kHz (Digidata 1440A; Molecular Devices; Sunnyvale, CA) and recorded using AxoScope (version 2.0.14) software. The visual stimulus computer sent a TTL pulse to the recording computer indicating each stimulus change.

Spike sorting.

Digitized spike traces were analyzed offline with Spike2 for Windows software (Cambridge Electronic Design; Cambridge, UK) and Matlab (R2014b; MathWorks; Natick, MA). Single units were classified offline using the spike sorting program in Spike2. Spikes (wave-marks) were extracted from the raw trace (waveform) using full-wave templates created using two trigger thresholds to exclude noise and capture spikes. The template window was expanded to encompass the full spike; 60% of points in the spike had to match a given template in order to be added to that template code. Similar templates were grouped together using PCA cluster analysis.

Visual stimulus presentation.

Neurons in the LM are identifiable based on their high levels of spontaneous activity and motion sensitivity. They are selective for direction, velocity and size of large-

field visual stimuli [S7,S23–S25]. Direction selectivity was initially assessed using a handheld stimulus (random black pattern on white board) moved in several directions in the contralateral visual field at a range of speeds. Once a responsive site was isolated, a computer monitor (144 Hz, 83° X 53°, ASUS) was positioned 30 cm away and tangent to the viewing eye for stimulus presentation. LM neurons have large receptive fields that can encompass the entire visual hemifield [S24,S26]. Therefore, we attempted to center the monitor in the cell's receptive field. To test the response properties of LM cells to visual motion, two stimulus programs were created using Psychophysics Toolbox-3 [S27–S29] in Matlab. The first program generated a plane of randomly positioned black dots (2.1° diameter) on a white background, covering the entire screen. The dots were moved at 36°/s in eight directions 45° apart, with the bill at 0°. In addition, in some cases, the dots were moved at 1°/s, though these recordings were ultimately not used in the preferred direction analysis. Each sweep consisted of 5 s of motion, followed by a 5 s pause, in each of the eight directions, and five sweeps were recorded at each site. Peristimulus time histograms (PSTHs; bin size = 250 ms) were generated for each 5 s stimulus. We generated a polar plot showing the directional tuning curve for each LM neuron by averaging the firing rate in each of the eight tested directions and fitting a B-spline function to these points. To determine whether a cell had a preferred direction we started with Rayleigh's test for uniformity. If a cell's responses were found to be non-uniform ($P < 0.05$), we determined a preferred direction for each cell by calculating a mean vector using the following equation, where FR = firing rate and n = the eight directions of motion (Graham and Wylie 2012):

$$Preferred\ direction = \tan^{-1}\left(\frac{\sum_n (FR_n \times \sin\theta_n)}{\sum_n (FR_n \times \cos\theta_n)}\right)$$

The mean vector calculation was matched with a maximum likelihood method to estimate parameters for a circular von Mises distribution to the firing data. These distributions are like normal distributions that can wrap around to accommodate circular data. Two parameters are estimated: a center for the distribution, μ and a concentration, κ that have similar meaning to the mean and standard deviation values for normal distributions. Both estimates give almost identical results for preferred direction.

Neurons were considered to be in the LM if they were spontaneously active and exhibited non-uniform excitation in response to motion in a “preferred direction.” Typically, this was accompanied by suppression in the “anti-preferred direction.” This response distinguishes LM cells from neighboring visual regions, such as the optic tectum and nucleus rotundus [S30].

We examined whether hummingbirds and zebra finches differ in the specificity of their response to direction, in other words, the width of the tuning curve (Figure S2). At thresholds less than 70% of the maximum firing rate, zebra finches have a narrower direction tuning width than hummingbirds. At angles greater than 45° from the preferred direction, a greater proportion of the zebra finch and pigeon LM cell population is closer to the spontaneous firing rate, meaning they are more narrowly tuned to direction than hummingbirds (Figure S2c-d). However, at the preferred direction ± 45°, there is no difference in direction tuning between the two species.

Once a preferred direction was established, a velocity tuning curve was generated for each neuron using a second Matlab script. The same random dot pattern used for direction tuning was used, but the dots were moved at a series of randomly presented speeds (0.24, 0.5, 1, 2, 4, 8, 16, 24, 32, 48, 64, 80°/s). Each sweep consisted of randomly interspersed trials in which dots were moved in the preferred or anti-preferred direction at each speed (5 s of motion followed by a 5 s pause; trials randomly selected without replacement). All dots were moved coherently at a constant speed. Neuronal spikes were analyzed by calculating the mean firing rate from 5 sweeps for each speed in both directions.

To quantitatively analyze the responses of LM neuron populations in hummingbirds and zebra finches to increasing motion speed, we fitted sigmoidal curves to normalized firing data from the velocity tuning curves. The sigmoidal function:

$$\text{response (speed)} = \frac{\text{a}}{1 + e^{-\text{s} * (\text{speed}-\text{c})}}$$

has three parameters: a is the upper asymptote, s is the slope, and c is the inflection point. Two separate models were fit to data from each species where either slope (s) or inflection point (c) were varied with a random effect of cell within site within track within bird. These two variations created a set of slopes and inflection points that could then be compared to determine differences between hummingbird and zebra finch LM responses to different motion speeds.

Statistical Analyses.

We examined the directional properties of 152 zebra finch LM units and 88 hummingbird LM units using a moving plane of random dots. We compared these data to the direction preferences of 100 pigeon LM units tested with drifting sine gratings. We used the Rayleigh test and von Mises distribution values for data from each species to analyze preferred direction bias at the cellular and population levels. Individual LM neurons included in the results analyses had to have a non-uniform distribution of firing rates in response to motion, and thus a preferred direction. In addition, to be included in the speed tuning width and speed preference analyses, LM neurons had to be tested in their preferred direction during the velocity tuning stimulus. Because cells within recording sites could only be isolated and analyzed for preferred direction after the experiment was completed, some cells were excluded from the velocity tuning analysis on this requirement.

All statistical analyses were performed on mean firing rates using R 3.1.2. Firing rates for each cell were normalized to the mean spontaneous firing rate for that cell. The average spontaneous firing rate for all LM cells was 31.6 Hz (± 3.0 SEM) for hummingbirds and 25.3 Hz (± 1.9) for zebra finches. In the preferred direction, the firing rate increased by 12.8 Hz (± 2.2) on average in hummingbirds and by 22.8 Hz (± 2.1) in zebra finches. Motion in the anti-preferred direction caused a decrease in the firing rate of 4.6 Hz (± 1.3) in hummingbirds and an increase of 0.9 Hz (± 0.9) in zebra finches. We analyzed circular distributions for preferred direction data using the circular package 0.4-7. We analyzed velocity tuning data using mixed effects regression models in the

nlme package 3.1-118, with a random effect of cell nested within site within track within individual to account for non-independence of repeated measures. Preferred direction (Figure S2), velocity tuning width (Figure S3D), preferred velocity (Figure S3G) and area under the curve (Figure 4) data were bootstrapped to obtain confidence intervals. We bootstrapped the data within each species by randomly sampling with replacement the responses of each cell to each stimulus treatment. Each cell was simulated 1000 times to generate 1000 LM populations. Hypotheses were evaluated using the multcomp package 1.3-8, and P-values < 0.05 were considered statistically significant.

Histology.

India ink injections (50-100 nL) or BDA injections (1%, 4.5 μA, 7s on/7s off, 15 min, D1956 ThermoFisher) were made at the end of experiments to confirm recording sites. Animals were given a lethal dose of ketamine/xylazine (i.m.) and immediately transcardially perfused with 0.9% saline followed by 4% paraformaldehyde.

Supplemental References:

S1. Iwaniuk, A.N., and Wylie, D.R.W. (2007). Neural specialization for hovering in hummingbirds: Hypertrophy of the pretectal nucleus lentiformis mesencephali. J. Comp. Neurol. *500*, 211–221.

S2. Wylie, D.R., Kolominsky, J., Graham, D.J., Lisney, T.J., and Gutierrez-Ibanez, C. (2014). Retinal projection to the pretectal nucleus lentiformis mesencephali in pigeons (*Columba livia*). J. Comp. Neurol. *522*, 3928–3942.

S3. Goller, B., and Altshuler, D.L. (2014). Hummingbirds control hovering flight by stabilizing visual motion. Proc. Natl. Acad. Sci. U. S. A. *111*, 18375–18380.

S4. Dakin, R., Fellows, T.K., and Altshuler, D.L. (2016). Visual guidance of forward flight in hummingbirds reveals control based on image features instead of pattern velocity. Proc. Natl. Acad. Sci. *113*, 8849–8854.

S5. Ros, I.G., and Biewener, A.A. (2016). Optic flow stabilizes flight in ruby-throated hummingbirds. J. Exp. Biol. *219*, 2443–2448.

S6. Donovan, E.R., Keeney, B.K., Kung, E., Makan, S., Wild, J.M., and Altshuler, D.L. (2013). Muscle activation patterns and motor anatomy of Anna's hummingbirds *Calypte anna* and zebra finches *Taeniopygia guttata*. Physiol. Biochem. Zool. Ecol. Evol. Approaches *86*, 27–46.

S7. Wylie, D.R., and Crowder, N.A. (2000). Spatiotemporal properties of fast and slow neurons in the pretectal nucleus lentiformis mesencephali in pigeons. J. Neurophysiol. *84*, 2529–2540.

S8. Crowder, N.A., and Wylie, D.R. (2002). Responses of optokinetic neurons in the pretectum and accessory optic system of the pigeon to large-field plaids. J. Comp. Physiol. A Neuroethol. Sens. Neural. Behav. Physiol. *188*, 109–119.

S9. Crowder, N.A., Dawson, M.R.W., and Wylie, D.R.W. (2003). Temporal frequency and velocity-like tuning in the pigeon accessory optic system. J. Neurophysiol. *90*, 1829–1841.

S10. Crowder, N.A., Lehmann, H., Parent, M.B., and Wylie, D.R.W. (2003). The accessory optic system contributes to the spatio-temporal tuning of motion-sensitive pretectal neurons. J. Neurophysiol. *90*, 1140–1151.

S11. Crowder, N.A., Dickson, C.T., and Wylie, D.R.W. (2004). Telencephalic input to the pretectum of pigeons: an electrophysiological and pharmacological inactivation study. J. Neurophysiol. *91*, 274–285.

S12. Tobalske, B.W., Biewener, A.A., Warrick, D.R., Hedrick, T.L., and Powers, D.R. (2010). Effects of flight speed upon muscle activity in hummingbirds. J. Exp. Biol. *213*, 2515–2523.

S13. Clark, C.J., and Dudley, R. (2010). Hovering and forward flight energetics in Anna's and Allen's hummingbirds. Physiol. Biochem. Zool. PBZ *83*, 654–662.

S14. Chai, P., Altshuler, D.L., Stephens, D.B., and Dillon, M.E. (1999). Maximal horizontal flight performance of hummingbirds: effects of body mass and molt. Physiol. Biochem. Zool. PBZ *72*, 145–155.

S15. Ellerby, D.J., and Askew, G.N. (2007). Modulation of pectoralis muscle function in budgerigars Melopsitaccus undulatus and zebra finches *Taeniopygia guttata* in response to changing flight speed. J. Exp. Biol. *210*, 3789–3797.

S16. Tobalske, B.W., Puccinelli, L.A., and Sheridan, D.C. (2005). Contractile activity of the pectoralis in the zebra finch according to mode and velocity of flap-bounding flight. J. Exp. Biol. *208*, 2895–2901.

S17. Tobalske, B.W., Peacock, W.L., and Dial, K.P. (1999). Kinematics of flap-bounding flight in the zebra finch over a wide range of speeds. J. Exp. Biol. *202*, 1725–1739.

S18. Tobalske, B., and Dial, K. (1996). Flight kinematics of black-billed magpies and pigeons over a wide range of speeds. J. Exp. Biol. *199*, 263–280.

S19. Clark, C.J. (2009). Courtship dives of Anna's hummingbird offer insights into flight performance limits. Proc. R. Soc. Lond. B Biol. Sci. *276*, 3047–3052.

S20. Lisney, T.J., Wylie, D.R., Kolominsky, J., and Iwaniuk, A.N. (2015). Eye morphology and retinal topography in hummingbirds (Trochilidae: Aves). Brain. Behav. Evol. *86*, 176–190.

S21. Ritland, S.M. (1982). The allometry of the vertebrate eye.

S22. Euler, T., and Baden, T. (2016). Computational neuroscience: Species-specific motion detectors. Nature *535*, 45–46.

S23. Xiao, Q., and Frost, B.J. (2013). Motion parallax processing in pigeon (*Columba livia*) pretectal neurons. Eur. J. Neurosci. *37*, 1103–1111.

S24. Fu, Y.X., Gao, H.F., Guo, M.W., and Wang, S.R. (1998). Receptive field properties of visual neurons in the avian nucleus lentiformis mesencephali. Exp. Brain Res. *118*, 279–285.

S25. Ibbotson, M.R., and Price, N.S.C. (2001). Spatiotemporal tuning of directional neurons in mammalian and avian pretectum: A comparison of physiological properties. J. Neurophysiol. *86*, 2621–2624.

S26. Winterson, B.J., and Brauth, S.E. (1985). Direction-selective single units in the nucleus lentiformis mesencephali. Exp. Brain Res. 60, 215–226.

S27. Kleiner, M., Brainard, D., Pelli, D., Ingling, A., Murray, R., Broussard, C., and others (2007). What's new in Psychtoolbox-3. Perception *36*, 1.

S28. Pelli, D.G., and Farell, B. (1995). Psychophysical methods. Handb. Opt. *1*, 29–1.

S29. Brainard, D.H. (1997). The psychophysics toolbox. Spat. Vis. *10*, 433–436.

S30. Frost, B.J. (2010). A taxonomy of different forms of visual motion detection and their underlying neural mechanisms. Brain. Behav. Evol. *75*, 218–235.